Accurate staging of reproduction development in Cadenza wheat by non-destructive spike analysis.

José Fernández-Gómez*, Behzad Talle, Alison Tidy and Zoe A Wilson*

jose.fernandez@nottingham.ac.uk

behzad.talle@nottingham.ac.uk

alison.tidy@nottingham.ac.uk

zoe.wilson@nottingham.ac.uk

School of Biosciences, University of Nottingham, Sutton Bonington Campus, Loughborough, Leicestershire, LE12 5RD, UK

*To whom correspondence should be addressed.

Tel: +44-115-9513235; Fax: +44-115-9516334;

Email: zoe.wilson@nottingham.ac.uk; jose.fernandez@nottingham.ac.uk

Keywords: barley, growth staging, anther, pollen development, Zadoks stage, Last Flag Elongation.

Running Title: Non-destructive staging of reproduction development staging in Cadenza wheat

Highlight: Non-destructive staging of reproduction development in Cadenza, using a double-scale system whereby anther/pollen development can be predicted in relation to spike size and spike position within the pseudostem.

Date of submission: 21-05-2019

Number of Figures: 6

Number of Tables: 1

SUMMARY

Wheat is one of the most important crops in the world, however, loss of genetic variability and abiotic stress caused by variable climatic conditions threaten future productivity. Reproduction is critical for wheat yield, however pollen development is amongst the most sensitive developmental stage to stresses such as heat, cold or drought. A better understanding of how anther and pollen development is regulated is needed to help produce more resilient crops and ensure future yield increases. However, in cereals such as wheat, barley and rice, flowers form within the developing pseudostem and therefore accurate staging of floral materials is extremely challenging. This makes detailed phenotypic and molecular analysis of floral development very difficult, particularly when limited plant material is available, for example with mutant or transgenic lines. Here we present an accurate approach to overcome this problem, by non-destructive staging of reproduction development in Cadenza, the widely used spring wheat research variety. This uses a double-scale system whereby anther and pollen development can be predicted in relation to spike size and spike position within the pseudostem. This system provides an easy, reproducible method that facilitates accurate sampling and analysis of floral materials, to enable anther and pollen developmental research.

INTRODUCTION

Wheat is one of the main staple foods worldwide and is the most abundant crop cultivated in the developing world, providing 20% of total dietary calories and proteins worldwide (Shiferaw *et al.*, 2013), however loss of genetic variability due to domestication and abiotic stress caused by variable climatic conditions threaten future productivity (Smýkal, 2018). Wheat yearly production reached 14.1 mTns, with a total market value of 2.63 billion dollars in 2016 (Rabobank, 2016). However, increasing populations and a steady growth in wheat consumption alongside climatic variability, means that wheat yields need to increase by an

estimated 2.6% per annum to meet ongoing demand (Shiferaw *et al.*, 2013), which poses major challenges for breeders, researchers and governments. In addition, the exhaustion of the effects that increased wheat yield during the green revolution (Whitford *et al.*, 2013) and new environmental policies, mean that novel varieties capable of contributing to more sustainable and resilient crops are needed (Shiferaw *et al.*, 2013).

Multiple factors contribute to yield loss, from impoverishing of genetic variability due to intensive farming and domestication, and a/biotic stresses. To help mitigate these adverse effects, introgression programmes are ongoing to introduce beneficial traits that were lost due to intensive farming and domestication, from ancestors into modern elite lines (Grewal *et al.*, 2018). In addition, new genomic tools have been developed to exploit the potential within the wheat genome. For example, genome sequencing, transformation, gene editing and genomic tools, are facilitating more ambitious research into wheat yield sensitivity to a/biotic stresses (Dolferus *et al.*, 2011; Liu *et al.*, 2015; Parish *et al.*, 2012). Research carried out in *Arabidopsis* and rice has shown that stress can impair reproduction, particularly during meiosis, gametogenesis and fertilization (Barnabas *et al.*, 2008); for instance, drought (Ding *et al.*, 2018), heat or cold stress (Zampieri *et al.*, 2017) causes abnormal pollen development reducing fertility (Shimono *et al.*, 2016). The impact of stress damage is also particularly dependant on the stage when it occurs and the species. For instance, stress during pollen development in rice, when the tapetum activity is high during the transition between tetrads to early microspore release, produces major damage (Chaturvedi *et al.*, 2017; Oliver *et al.*, 2005).

However, research on flower development, fertility regulation and associated sensitivity to environmental stress in wheat, is significantly limited by the accurate staging of anther and pollen development. From early reproductive development until spike emergence floral development occurs within the pesudostem, and thus is not visible without destructive analysis. This means that it is extremely difficult to accurately stage and collect floral samples for phenotypic or molecular analysis without damaging the plant, this is particularly important when limited plant resources are available, for example for mutant or transgenic lines. It is therefore necessary to develop staging systems based on overall plant morphology and development that can be linked to anther and pollen development, instead of using

samples collected based on plant age (Ninkovic and Åhman, 2009; Simmons *et al.*, 2006). Non-destructive prediction methods are preferable to conventional anther or floret measurement that require plant dissection (Gómez and Wilson, 2012).

The prediction of anther and pollen development has been approached in different manners; generally anther and pollen stages appear to be tightly linked to spike and anther size in barley and wheat (Kirby, 1988; Waddington *et al.*, 1983). Waddington et al. (1983) developed a scoring system for barley and wheat that correlates spike development with anther length. In addition, other studies correlate floret size and anther length with stages of anther development in rice (Raghavan, 1988). Recently a study of four Australian wheat varieties has shown that spikelet and anther size can be used to accurately predict anther stages (Browne *et al.*, 2018). However, these systems require the dissection of plants to measure the parameters used to predict the anther and pollen development stages and therefore are not suitable for ongoing developmental analyses. Gomez and Wilson (2012) previously developed a non-destructive staging system in barley based upon the Zadok stages, that combined node number, Last Flag Elongation (LFE) and ear position within the plant to predict spike size in barley, which was then linked to anther and pollen development stages (Gómez and Wilson, 2012). In addition, a non-destructive method of measuring the auricula distance (distance between the auricles of the flag leaf and the penultimate leaf) has been used in wheat and rice to predict the young microspore stage (Ji *et al.*, 2010; Morgan, 1980; Oliver *et al.*, 2005), however this approach is varietal specific and has limitations in its ability to predict all anther stages.

Here we present a non-destructive anther and pollen development staging system in the wheat variety Cadenza. Cadenza is a widely used research variety that was the genotype selected to generate the wheat Tilling Exon Capture Population (King *et al.*, 2015). This publicly available population contains thousands of mutant lines, which have annotated gene mutations that are available for public use (https://www.seedstor.ac.uk/shopping-cart-tilling.php). The development of this prediction system will enable accurate analysis of anther and pollen development which combined, with the availability of this mutant population, will allow ambitious research programmes on reproductive development.

MATERIALS AND METHODS

Plant materials

Spring wheat variety Cadenza was grown under controlled conditions of 18ºC/14ºC and 16 hours photoperiod (80% RH, 500 µmol/m2/s metal halide lamps (HQI) supplemented with tungsten bulbs). Seeds were sown in 12 well (80 ml each) pots using John Innes Nº 3 compost (https://www.gardenhealth.com/j-arthur-bowers-john-innes-3-compost). After 2-3 weeks (Zadoks stage 11-12: one shoot with 1 or 2 unfolded leaves), plants were transferred to 5 litre pots containing Levington CNS compost (90N 46P 150K) with 3 plants per pot. Plants were fed once after being transferred to 5 litres pot with Osmocote Exact Tablets (5 gr; 16-9-12+2MgO+TE; http://icl-sf.com).

Morphological Analysis

Cadenza morphological development was studied from the onset of the elongation stage to anther anthesis to gain better understanding of Cadenza development and to establish clearly recognisable features that could be related to anther development. Zadoks decimal code was initially used to identify key developmental points (Zadoks *et al.*, 1974), however, new time points were used to establish a correlation between morphological and reproductive development. Five plants, with four tillers per plant, were used. Material used for data collection was restricted to tillers that were already within the elongation stage when the main shoot was around booting stage. The florets analysed were collected from spikelet position 1 and 2, and always in the central positions within the spike (Figure 1c). Data was collected every three days and consisted of: total height, number of nodes, internode elongation, flag leaf emergence (shoot axis elongation), spike position within the pseudostem, spike emergence, peduncule elongation after total spike emergence and spike size (Figure 1).

In addition, a separate replicate set of plants growing under the same conditions were used for spike size analysis. All the data parameters were collected, however, these plants were dissected to measure the spike and to collect anther samples for sectioning and qRT-PCR. Further generations of material were also subsequently grown for analysis and confirmation of the staging system.

Histological analysis of anther development

Florets from the middle zone of the spike were collected from different spike developmental stages. Floral buds from different stages were fixed overnight in 4ºC in 4% (v/v) paraformaldehyde. Tissues were washed twice (30 min each) with 1xPBS. Fixed panicles were immediately dehydrated with ethanol (30-100% (v/v)) prior to embedding in Spurr resin (TAAB Laboratories Equipment, Ltd). After 100% ethanol, samples had a mixture of ethanol 100% and Ox.propilene (Sigma) 1:1 added, which was replaced by 100% Ox.propilene after 20 min. As a pre-infiltration step, samples were mixed with Ox.propilene/Spurr resin (1:1) for 1.5 hours, the solution was then replaced with 100% Spurr resin and kept at 4°C overnight. After this, samples were embedded in molds using Spurr resin and incubated at 70-75°C for 10-12hr. Ultrathin sections (0.5µm) were produced using an ultramicrotome Leica EM UC6. Sections were stained with 0.25% (w/v in 1% Sodium Borate) toluidine blue prior to imaging.

Anther specific gene expression

Due to the high specificity of some of the genes expressed in the anther development network, expression analysis was used as an additional approach to confirm the correlation between the samples collected and the expected stages. Samples were collected using spike size/position scale covering all spike stages. RNA was purified using RNeasy spin columns (Qiagen). First-strand cDNAs were synthesized from1.5 µg total RNA using Superscript III reverse transcriptase (Invitrogen) and an oligo (dT) primer (Invitrogen) according to the manufacturer's instructions. Three anther specific genes were used for staging, *TaDYT1, TaMS1* and *TaMYB26*. TaDYT1 and TaMS1 are essential tapetum specific transcription factors, whereas TaMYB26 plays a critical role in anther dehiscence.

X-ray µCT Scanning

X-ray µCT scanning of wheat plants were performed using the v|tome|x M 240 kV X-ray µCT scanner (GE Sensing & Inspection Technologies GmbH, Wunstorf,

Germany). Scanning conditions were 80kV voltage, 250 current, 250 timing, 32 average, 0 skips, 1x1 bining and 4.0 sensitivity. A single radiograph consisting of 32 integrated images was taken to limit the X-ray dose to the plant to 10s per radiograph (total exposure 15 minutes over all scans). Spikes and nodes were easily identifiable by this method, and close up images of each spike being monitored were taken, as well as an overall picture. Three plants were taken from early flowering, and individual tillers were identified and monitored over 2 weeks (Day 0, 7 and 14) to monitor spike growth and position (Tracy *et al.*, 2017).

RESULTS

Plant morphology development in wheat variety Cadenza

Plant development was studied to establish a correlation between external morphology and anther developmental stages for the wheat cultivar Cadenza (Figure 1). In order to gain knowledge about Cadenza's external morphological development, the emergence of nodes and the internode elongation were noted and total tiller height and last flag elongation were measured (Figure 2). In addition, spike position within the pseudostem and its relationship with spike size was determined (Figure 3-4; Table 1). Finally, a system that relates spike size/positioning within the plant and anther staging was established (Figure 4-5) (Table 1).

Internode and Last Flag Leaf (LFE) elongation development

Nodes and internode elongation, total tiller height and last flag elongation (LFE) data were collected every three days from the two detectable nodes until spikes were out and the peduncule extended (Figure 2). Data collected permitted the creation of 5 internode stages based on nodes visability and internode elongation (Figure 2, 3a (red bracketed regions), which were also confirmed by μCT analysis (Figure 3). Three main stages (1, 3 and 5), and two intermediaries (2 and 4) were created encompasing all points of reproductive development (Figure 2). At internode stage 1, internodes 1 and 2 were fully elongated, whereas at stage 3, the three first internodes were fully elongated, plus the fourth was elongated only a quarter of its expected maximum (Figure 2). Finally by internode stage 5 all internodes (1-4) had reached maximum elongation (Figure 2). To increase

accuracy, two intermediary stages were included which recorded the production of internodes between the main stages (Figure 2). At stage 2, the first two internodes had elongated fully and the third only to half of its expected maximum (Figure 2), whilst at stage 4, the first three internodes were fully elongated and the fourth had elongated to three quarters of its expected maximum (Figure 2).

Tiller height was measured from the plant base, until the last visible auricle (Figure 1b). Height increase progressed steadily from 32.75 cm at internode stage 1, until 65.07 cm at internode stage 5 (Figure 2). Last Flag Elongation (LFE) was measured from its first appearance between internode stage 1 and 2, until the end of plant development at internode stage 5 (Figure 1a; Figure 2). LFE showed a constant elongation until internode stage 3 (Figure 2a), after which it remained unaltered until the end of tiller development (Figure 2).

Spike upward movement and development within spike

From the start of the reproductive stage (first node detectable separated >1cm from the ground) (Zadoks *et al.*, 1974), the spike starts an upward movement driven by internode elongation that continues until the spike is completely emerged and the peduncle stops elongating (Figure 4a). This spike upward movement was divided into 16 identifiable points (spike stages) (Figure 4a; Table 1). These spike stages started from the point at which the spike was completely in PLS1 (Prior to previous Last Sheath) (Figure 4a, spike stage 1). Five more stages (2-6) were established describing the spike upward movement between PLS1 and PLS (Previous Last Sheath) (Figure 4a). Stages 2 and 3 reflect the transition within the PLS1, entering into PLS at stage 4. Spike upward movement within PLS continued between stages 5 and 6, just before entering the Last Sheath stage. From stage 6, five more stages were established describing the spike's movement within the Last Sheath (LS) (stages 7-11) (Figure 4a). From stage 7 (spike one quarter within the LS) the spike moves upward to reach half way (stage 8), three quarters (stage 9), all within (stage 10) the last sheath. The internode extension subsequently pushes the spike further up within the leaf sheath, bringing the spike to the top of the leaf sheath immediately before emergence (stage 11, booting) (Figure 4a). From this point, and continuing until the spike emergence, five more stages were characerised:

spike one quarter emerged (stage 12), half way (stage 13) and three quarters out (stage 14), spike fully out (peduncule elongated between 0-3 cm, stage 15), and finally spike fully out with peduncule elongated over 3 cm (Figure 4a) (Table 1).

Spike stage correlation with spike size was determined by measuring spikes collected using our spike staging system (Figure 4b; Table 1). Spikes showed a continuous growth from Zadok stage 30, spike around 0.5 cm (sample day 1, Figure 3b) and could be easily linked to spike position from spike stages 1 (1.5+/-0.3 cm) until stages 9-10 (9.5+/-0.4 cm) (Figure 4b; Table 1). After stage 9 the spike reached its maximum size (10-11 cm), remaining unchanged until the end of development at stage 16 (Figure 4b).

The combination of spike size and its position within the pseudostem can be used to predict anther development

To establish a correlation between spike size/position and anther development, spike staging was used to collect different spike samples for ultra-thin microscopy. Due to the spike ceasing to grow from stage 9 onward (Figure 4b), spike size prediction was used to collect samples from stage 1-9, whereas spike position was used between stages 10-16 (Figure 4-5).

Anther transverse sections showed a close relationship between spike size/position and anther stage (Figure 4-5; Table 1). Anthers collected at stage 1 (spike ~1.4 cm) showed three anther layers (Epidermis, Endothecium and Middle layer) and sporogenous cells occupying the central locule (Figure 5a). Between stages 2 and 3, the sporogenous cells continued dividing and the tapetum became apparent (Figure 5, spikes 2.1-3 cm). At stage 3-4, all four anther layers were clearly visible and microspore mother cells (MMC) were formed (Figure 5, spike 3-3.9 cm). MMC entered into meiosis at stage 4 (Figure 5, spike 4.7 cm) and by stage 6 early tetrads were visible (stage 6, ear 6.2 cm, Table 1). Tetrad stage continued until stage 7-8 (Figure 5, spike 7.3 cm). Between stages 6-8 the middle layer started to disappear (Figure 5). At stage 9-10, young microspore were released from tetrads, with no middle layer observed (Figure 5; spike 9 cm). Vacuolated microspores and pollen grains were visible at stages 11-12, the tapetum started to degenerate between stages 10-11 coinciding with the release of microspores and the formation

of vacuolated microspores (Figure 5). Pollen Mitosis I occurred at stage 13-14 (Figure 5), the tapetum layer was still partly present. Stage 16 showed septum lysis leaving two anther locules prior to anther dehiscence (Figure 5).

This combined staging approach allowed the identification of critical anther development stages using easily identifiable spike size and positioning within the pseudostem stages (Figure 4) (Table 1). The system was divided into two parts due to the spike ceasing to grow after stage 9. From stages 1 to 9, spike size as determined using spike position, was used to predict anther development progression. This allowed the identification of critical stages for male fertility such as tapetum formation (stages 2-3), meiosis (stages 4-5) and tetrad formation (stages 6-8) (Figure 4-5). From stages 10-16, samples were selected only based on spike position, identifying stages from young microspore release (stage 9) until anthesis (stage 16) (Figure 4-5).

Anther and pollen specific expression corresponds to expected developmental staging

A non-destructive accurate anther and pollen development staging system is critical to study male fertility, to perform gene expression profiles, mutant expression analysis or RNAseq sample collection. Therefore, sampling accuracy is vital. To test the accuracy of our staging method (based upon spike size and position) in predicting anther development stages, three highly anther specific transcription factors, MS1, MYB26 and DYT1, were selected for gene expression analysis. These three transcription factors have been characterised in *Arabidopsis*, rice and barley, and are involved in pollen formation (MS1 and DYT1) and anther dehiscence (MYB26). The three wheat orthologues were found using barley equivalent sequences by comparative analysis against wheat database (https://plants.ensembl.org/Triticum_aestivum/Info/Index) (Supplementary Figure 1). Expression was analysed using primers that amplify the three homologues simultaneously (Supplementary Table 1).

MS1 in Arabidopsis, rice and barley is expressed in the tapetum just before microspore release as the callose surrounding the tetrad starts to breakdown until the free microspore stage (Fernandez Gomez and Wilson, 2014; Li *et al.*, 2011;

Wilson *et al.*, 2001). MYB26, a transcription factor that regulates secondary thickening in the endothecium and is essential for anther dehiscence, is expressed just before Mitosis I until Bicellular pollen stage (Yang *et al.*, 2007). Finally *UDT1*, the Arabidopsis *DYT1* orthologue in rice, shows a bimodal expression pattern with two expression peaks, at meiosis and at early tetrad stage (Jung *et al.*, 2005). The expression patterns of the putative wheat orthologues showed similar profiles to those observed in *Arabidopsis*, rice and barley. *TaMS1* expression was observed in anthers between early tetrad to vacuolated pollen stage, reaching maximum expression at early microspore release (Figure 6a). Furthermore, *TaMYB26* showed maximum expression between vacuolated pollen and Mitosis I stage (Figure 6b). *TaDYT1* showed low expression from sporogenous cells (SC) to sporogenous cells-tapetum generation (SCt) stages, increasing at the free microspore stage (Ms), then decreasing again at the microspore-tapetum transition stage (MC-Tt). From MC-Tt, expression reaches its peak at early tetrad stages (ETd), decreasing again around young microspores (Ym) increasing slightly at Mitosis I (Figure 6c). These results confirm the accuracy of the non-destructive staging system for collection of stage specific samples, enabling higher precision in sample collection which is needed for detailed molecular and physiological analysis of pollen development.

DISCUSSION

Cadenza development

Predicting anther and pollen development stages is key to investigate plant fertility, the sensitivity of this critical trait to environmental stress and the potential generation of hybrid seeds. Facilitating effective sample collection can also contribute to more homogeneous sampling sets in experiments such as RNAseq, or expression analysis, that will facilitate the identification and characterisation of genes of interest and their manipulation.

Wheat cultivar Cadenza has been extensively used as a research tool, and recently, a multinational effort has generated an Exon Capture Population that is contributing to accelerate wheat research (King *et al.*, 2015). Therefore, this variety is a good model for developmental studies and the generation of a system for accurate anther staging will capitalise on the existent mutant population and

contribute to male fertility gene characterisation. Physiological measurements, destructive staging using sectioning, and non-destructive staging were all used to generate combined data on the progression of Cadenza flower development. X-ray μCT contributed to the analysis of spikes at a very early stage in development (spike < 1 cm; undifferentiated tissue) to assist in the developmental assessment and in additional validation of our final staging system (Figure 3).

Wheat anther staging has been studied in detail by Mizelle et al (1989), however, no relationship between external development and anther development was established (Mizelle *et al.*, 1989). Nonetheless, attempts to establish relationships between spikelet and anther sizes have proven very accurate in predicting these stages (Browne *et al.*, 2018; Kirby, 1988; Waddington *et al.*, 1983), however, these systems require plant dissection and therefore destruction of the plant materials.

Non-destructive methods based on auricle distance (AD) have been used in rice (Oliver *et al.*, 2005) and wheat (Ji *et al.*, 2010) to predict young microspore stage in cold and drought stresses treatments. However, the relation between auricle distance (AD) and anther stages in wheat proved highly varietal specific (Browne *et al.*, 2018). This was confirmed in Cadenza where LFE (denomination used instead of AD in this paper) proved to be inadequate to predict all anther stages due to the early cessation of elongation observed in the last flag around spike stage 9-10 (Figure 2).

Parallelism between pseudostem and spike development has been described previously during wheat elongation stages (Kirby, 1988; Reynolds *et al.*, 2009) and a correlation was made between increase in spike size and floret development scores (Waddington *et al.*, 1983). However, establishing a relationship between external morphological changes, spike size and anther stages is difficult due to varieties differences and by the ongoing spike development within the pseudostem. In barley, this relationship between external characters and spike sizes/anther stages was successfully established (Gómez and Wilson, 2012) by modification of the traditional Zadok developmental scale (Zadoks *et al.*, 1974) and the introduction of additional marker stages. Clear prediction of spike size was possible for most stages of barley floral development; however, as the spike stopped growing just after the last flag started to elongate, a combination of last flag elongation and spike position within the plant was adopted to increase the

accuracy of stage identification (Gómez and Wilson, 2012). As in barley, Cadenza's spike reached a maximum size around spike stage 9-10 (Figure 4b), at the point when the spike is entering the last sheath and microspores have been released from tetrads (Figures 5-6). After this point, prediction of stage based on spike size alone can not discriminate between these critical anther developmental stages (Figures 4-5 Table 1).

Anther stages prediction system

Internode elongation stages were initially targetted as the principal morphological parameter to link with anther development (Figure 2a), however this meant that predictions of internode maximum elongation were needed to establish the internode stages, which proved to be complex. Nonetheless, internode stages contributed to increasing the knowledge regarding Cadenza development and morphology. This knowledge facilitated the generation of a spike position staging which proved highly consistent and easy to follow as stated here and in previous investigations (Gómez and Wilson, 2012; Kirby, 1988; Reynolds *et al.*, 2009) (Figure 4; Table 1).

Spike size and its correlation with spike position resulted in a very accurate prediction of anther development stages (Table 1). As in barley (Gómez and Wilson, 2012), wheat spike size was valuable to predict anther and pollen development, at least until stages where the spike ceased growing (spike stage 9; Figure 4; Table 1). From this point, anther staging prediction was continued by using the spike position within the leaf sheath which showed a clear correlation to anther stages until anther dehiscence (stages 10-16; Figures 4-5; Table 1). Therefore, this double scale facilitated the identification of the stages from the onset of plant reproduction until anthesis (Figures 4-5); this provides a tool for accurate sample collection aimed at analysing gene expression and developmental characterisation (Figure 6; Table 1). This staging system was confirmed using μCT and qRT-PCR expression analysis of key anther-specific genes; this validated the staging system, but is not required for subsequent accurate analysis staging of materials.

Similar anther and pollen development progress was observed in wheat and barley (Figure 5b), however differences were observed in their timing and duration. For instance, in barley, stages such as tetrads and young microspore release occurred earlier in plant development, before all nodes were detected and extended (barley stage 33-34), and spikes were between 2.5-4.5 cm (Gómez and Wilson, 2012). In addition, these important stages all occurred before the last flag had started elongating (Gómez and Wilson, 2012) (Figure 5b). On the other hand, in wheat, early tetrad stage occurred at spike stage 5-6 when spikes were over 6 cm long and the spike was about to enter the last flag sheath, which is already elongated to over 8 cm (Figure 4) (Table 1). Moreover, it was observed that wheat tetrad stage lasted longer than in barley (Figure 5b). In wheat, meiosis was observed at spike stage 4-5 (spike around 4.5cm), with tetrads evident soon after (stage 5-6, spike around 6.2cm) (Table 1), and lasting until stage 8 (spike 7-8 cm). These stages corresponded to spike stages just before entering the last sheath (stage 6) until the spike was half within the spike (stage 8) (Figure 4). Whereas, the tetrad stage in barley was much quicker, lasting from spike 3-4 cm (Gómez and Wilson, 2012), or Zadoks stages 33-33.5 (Zadoks *et al.*, 1974) (Figure 5b). Environmental conditions and genotype is likely to impact upon developmental progression and slight variation has been seen between different wheat genotypes (data not shown). Our floral staging system was developed for Cadenza grown under controlled environment condition since it is extensively used as a model for wheat molecular genetic analysis, nevertheless this staging system provides a basis for direct application to other wheat genotypes and growth conditions, and can be readily correlated to other wheat genotypes/growth conditions.

This system of using spike size and position to determine anther development stage, was further validated by expression analysis of three anther/stage specific transcription factors, *TaMS1*, *TaMYB26* and *TaDYT1* (Jung *et al.*, 2005; Wilson *et al.*, 2001; Yang *et al.*, 2007). Samples collected using the spike size/position staging system were analysed by RT-qPCR (Figure 6) to confirm the stages. Expression analysis for the three wheat genes were similar to the expression of their orthologues in *Arabidopsis* (Wilson *et al.*, 2001; Yang *et al.*, 2007), rice (Jung *et al.*, 2005; Li *et al.*, 2011) and barley (Fernandez Gomez and Wilson, 2014). Some differences were observed in the MYB26 expression pattern that is restricted

to early Mitosis I until Bicellular pollen in Arabidopsis (Yang *et al.*, 2007), whereas in wheat, expression seems to be more widespread through the development (Figure 6b). This confirms the accuracy of this staging system to predict anther development by a non-destructive method in Cadenza. This method, although focussed upon Cadenza growing under control conditions, provides a valuable tool for anther and pollen stage prediction that will contribute to increased understanding of male fertility by enabling correct sampling of materials to facilitate gene expression analysis, RNAseq sampling and gene characterisation.

SUPPLEMENTARY DATA

Supplementary Figure 1. Inter-species similarities between the three anther transcription factors used for expression analysis. a) NCBI Blast (https://blast.ncbi.nlm.nih.gov/Blast.cgi) was used for alignment between the Arabidopsis-Rice and barley, whilst EnsemblePlants was used to find the similarities between the barley orthologue and wheat homologues. b) Phylogenetic trees generated for the transcription factors.

Supplementary Table 1. Primers used for qRT-PCR analysis of wheat anther-specific transcription factors.

ACKNOWLEDGEMENTS

This work was supported by the Biotechnology and Biological Sciences Research Council and AHDB [project number D-21130024], KWS UK Ltd, Limagrain UK Ltd, RAGT Seeds Ltd. and SECOBRA Recherches as part of a LINK grant [grant number BB/P002080/1].

REFERENCES

Barnabas B, Jager K, Feher A. 2008. The effect of drought and heat stress on reproductive processes in cereals. Plant, Cell & Environment **31**, 11-38.

Browne RG, Iacuone S, Li SF, Dolferus R, Parish RW. 2018. Anther Morphological Development and Stage Determination in Triticum aestivum. Frontiers in Plant Science **9**.

Chaturvedi AK, Bahuguna RN, Shah D, Pal M, Jagadish SVK. 2017. High temperature stress during flowering and grain filling offsets beneficial impact of elevated CO(2) on assimilate partitioning and sink-strength in rice. Scientific reports **7**, 8227-8227.

Ding J, Huang Z, Zhu M, Li C, Zhu X, Guo W. 2018. Does cyclic water stress damage wheat yield more than a single stress? PLOS ONE **13**, e0195535.

Dolferus R, Ji X, Richards RA. 2011. Abiotic stress and control of grain number in cereals. Plant Science **181**, 331-341.

Fernandez Gomez J, Wilson ZA. 2014. A barley PHD finger transcription factor that confers male sterility by affecting tapetal development. Plant Biotechnol J **12**, 765-777.

Gómez JF, Wilson ZA. 2012. Non-destructive staging of barley reproductive development for molecular analysis based upon external morphology. Journal of Experimental Botany.

Grewal S, Yang C, Edwards SH, Scholefield D, Ashling S, Burridge AJ, King IP, King J. 2018. Characterisation of Thinopyrum bessarabicum chromosomes through genome-wide introgressions into wheat. TAG. Theoretical and applied genetics. Theoretische und angewandte Genetik **131**, 389-406.

Ji XM, Shiran B, Wan JL, Lewis DC, Jenkins CLD, Condon AG, Richards RA, Dolferus R. 2010. Importance of pre-anthesis anther sink strength for maintenance of grain number during reproductive stage water stress in wheat. Plant Cell and Environment **33**, 926-942.

Jung K-H, Han M-J, Lee Y-S, Kim Y-W, Hwang I, Kim M-J, Kim Y-K, Nahm BH, An G. 2005. Rice Undeveloped Tapetum1 Is a Major Regulator of Early Tapetum Development. The Plant Cell **17**, 2705-2722.

King R, Bird N, Ramirez-Gonzalez R, Coghill JA, Patil A, Hassani-Pak K, Uauy C, Phillips AL. 2015. Mutation Scanning in Wheat by Exon Capture and Next-Generation Sequencing. PLOS ONE **10**, e0137549-e0137549.

Kirby EJM. 1988. Analysis of Leaf, Stem and Ear Growth in Wheat from Terminal Spikelet Stage to Anthesis. Field Crops Research **18**, 127-140.

Li H, Yuan Z, Vizcay-Barrena G, Yang C, Liang W, Zong J, Wilson ZA, Zhang D. 2011. PERSISTENT TAPETAL CELL1 Encodes a PHD-Finger Protein That Is Required for Tapetal Cell Death and Pollen Development in Rice. Plant Physiology **156**, 615.

Liu H, Searle IR, Mather DE, Able AJ, Able JA. 2015. Morphological, physiological and yield responses of durum wheat to pre-anthesis water-deficit stress are genotype-dependent. Crop and Pasture Science **66**, 1024-1038.

Mizelle MB, Sethi R, Ashton ME, Jemen WA. 1989. Development of the pollen grain and tapetum of wheat (*Triticum aestivum*) in untreated plants and plants treated with chemical hybridizing agent RH0007. Sexual Plant Reproduction **2**, 231-253.

Morgan JM. 1980. Possible Role of Abscisic-Acid in Reducing Seed Set in Water-Stressed Wheat Plants. Nature **285**, 655-657.

Ninkovic V, Åhman IM. 2009. Aphid acceptance of Hordeum genotypes is affected by plant volatile exposure and is correlated with aphid growth. Euphytica **169**, 177.

Oliver SN, Van Dongen JT, Alfred SC, Mamun EA, Zhao XC, Saini HS, Fernandes SF, Blanchard CL, Sutton BG, Geigenberger P, Dennis ES, Dolferus R. 2005. Cold-induced repression of the rice anther-specific cell wall invertase gene OSINV4 is correlated with sucrose accumulation and pollen sterility. Plant Cell and Environment **28**, 1534-1551.

Parish RW, Phan HA, Iacuone S, Li SF. 2012. Tapetal development and abiotic stress: a centre of vulnerability. Functional Plant Biology **39**, 553-559.

Rabobank. 2016. World Grain and Oilseeds Map. RaboResearch Agribusiness.

Raghavan V. 1988. Anther and Pollen Development in Rice (Oryza-Sativa). American Journal of Botany **75**, 183-196.

Reynolds M, Foulkes MJ, Slafer GA, Berry P, Parry MAJ, Snape JW, Angus WJ. 2009. Raising yield potential in wheat. Journal of Experimental Botany **60**, 1899-1918.

Shiferaw B, Smale M, Braun H-J, Duveiller E, Reynolds M, Muricho G. 2013. Crops that feed the world 10. Past successes and future challenges to the role played by wheat in global food security. Food Security **5**, 291-317.

Shimono H, Abe A, Aoki N, Koumoto T, Sato M, Yokoi S, Kuroda E, Endo T, Saeki KI, Nagano K. 2016. Combining mapping of physiological quantitative trait loci and transcriptome for cold tolerance for counteracting male sterility induced by

low temperatures during reproductive stage in rice. Physiologia Plantarum **157**, 175-192.

Simmons AT, Nicol HI, Gurr GM. 2006. Resistance of wild Lycopersicon species to the potato moth, Phthorimaea operculella (Zeller) (Lepidoptera: Gelechiidae). Australian Journal of Entomology **45**, 81-86.

Smýkal P, Nelson MN, Berger JD, Von Wettberg EJ. 2018. The Impact of Genetic Changes during Crop Domestication. Agronomy 8, 119-121.

Tracy SR, Gómez JF, Sturrock CJ, Wilson ZA, Ferguson AC. 2017. Non-destructive determination of floral staging in cereals using X-ray micro computed tomography (μCT). Plant Methods **13**, 9-21.

Waddington SR, Cartwright PM, Wall PC. 1983. A Quantitative Scale of Spike Initial and Pistil Development in Barley and Wheat. Annals of Botany **51**, 119-130.

Whitford R, Fleury D, Reif JC, Garcia M, Okada T, Korzun V, Langridge P. 2013. Hybrid breeding in wheat: technologies to improve hybrid wheat seed production. Journal of Experimental Botany **64**, 5411-5428.

Wilson ZA, Morroll SM, Dawson J, Swarup R, Tighe PJ. 2001. The Arabidopsis MALE STERILITY1 (MS1) gene is a transcriptional regulator of male gametogenesis, with homology to the PHD-finger family of transcription factors. Plant Journal **28**, 27-39.

Yang C, Xu Z, Song J, Conner K, Vizcay Barrena G, Wilson ZA. 2007. Arabidopsis MYB26/MALE STERILE35 regulates secondary thickening in the endothecium and is essential for anther dehiscence. Plant Cell **19**, 534-548.

Zadoks JC, Chang TT, Konzak CF. 1974. A decimal code for the growth stages of cereals. Weed Research **14**, 415-421.

Zampieri M, Ceglar A, Dentener F, Toreti A. 2017. Wheat yield loss attributable to heat waves, drought and water excess at the global, national and subnational scales. Environmental Research Letters **12**, 064008.

Spike stage	Description	Spike size	Anther stage
Stage 1	Spike starts PLS1	1.46 ± 0.26 cm	Four lobes formed. Sporogenous cells present. Three cell layers surrounding anther locule.
Stage 2	Spike middle PLS1	2.67 ± 0.5 cm	Sporogenous cells divide. Tapetum being formed.
Stage 3	Spike top PLS1, about to enter PLS	3.58 ± 0.16 cm	Microspore Mother Cells.
Stage 4	Spike one quarter within PLS		Microspore Mother Cells to Meiotic cells.
Stage 5	Spike all in PLS	4.33 ± 0.28 cm	
Stage 6	Spike all in PLS about to enter LS	6.6 ± 0.14 cm	Tetrads.
Stage 7	Spike one quarter within LS	7.36 ± 0.60 cm	
Stage 8	Spike half within LS		
Stage 9	Spike three quarters within LS	9.5cm	Young microspore release. Tapetum commences degeneration.
Stage 10	Spike all within LS	9.43 ± 0.4 cm	
Stage 11	Spike all within LS Booting	10.33 ± 0.28 cm	Vacuolated Microspore-Vacuolated Pollen. Tapetum visibly degenerating.
Stage 12	Spike one quarter out		
Stage 13	Spike half out	10.73 ± 0.87 cm	Vacuolated Pollen. Mitosis I start.
Stage 14	Spike three quarters out	10.9 ± 0.56 cm	Mitosis I.
Stage 15	Spike all out 0-3 cm	11.08 ± 0.58 cm	Mitosis II.
Stage 16	Spike all out elongated >3 cm	10.9 ± 0.45 cm	Anthesis.

Table 1. Spike position staging system. Spike size/position correlates accurately to anther development stages. From stage 1 to 9, spike continuously grew in size, however, from stages 9-10 stages, spike ceased growing. LS: Last Sheath; PLS: Previous Last Sheath; PLS1: Prior to Previous Last Sheath.

Figure Legends

Figure 1. Cadenza Last Flag Sheath development.

a) Three tillers at different stages of development showing different last flag sheath extension, sp indicates the spike position within the pseudostem. White circles show the nodes. b) Close up view of last flag and last sheath at three different elongation stages. c) Close up image of wheat spike indicating the middle area used for sample collection for sectioning and qRT-PCR. 1: PLS (Previous Last Sheath); 2: LS (Last Sheath); 3: Last Flag; 4: Auricle; sp: Spike Position; *: Spike middle region for sample collection; White arrows indicates spikelet 1 and 2 position, which were the only spikelets used for collection.

Figure 2. Cadenza morphological development.

a) Internode elongation stages were determined by measuring internode elongation every 3 days. Tiller height (green line) and last flag elongation (blue line) was also measured. b) Five internode stages were created, starting from two fully elongated internodes (interode stage1), until four fully elongated internodes (internode stage 5). Tiller height increased steadily from stage 1 until 5, reaching a maximum of 65.1 ±3.2 cm. Last Flag Elongation (LFE) appeared between stage 1 and 2 and reached maximum elongation at stage 3.

Figure 3. Cadenza internode and spike size development.

a) Internode elongation contribution to the spike upward movement (red brackets). b) Spike measurement started on day 48 after sowing (Zadock stage 30; spikes were around 0.5 cm long). a, c-e) μCT analysis of Cadenza spikelets. Spike size increase was observed over the following 14 days, spikes were up to 1.2 cm and >3 cm after 7 and 14 days respectively. c-e) Spike observed after c) day 1, d) day 7, and e) day 14.

Figure 4. Cadenza spike position stages and spike size/last flag elongation (LFE) progression.

a) Spike position was divided into 16 stages, from early development, just before spike enters the "prior to previous last sheath" (PLS1) spike stage 1, until the spike is completely emerged, peduncule is elongated and anthers enter anthesis (spike stage 16). These 16 stages were linked to spike position within the pseudostem. b) Spike stage/spike size correlation. Spike position and spike size showed a close correlation from stage 1 until stages 9-10. From stage 9-10 the spike ceased growing and remained unchanged.

Figure 5. Developmentally staged Cadenza anther transverse sections.

a) Stages 1-16 of Cadenza anther development. 1) Sporogenous stage; three anther layers are visible (arrow; Ep, En and ML), sporogenous cells occupy the central region of the locule. 2) Sporogenous cells divide. Three anther layers clearly visible; start of tapetum formation (T). 3) Microspore Mother Cells (MMC) evident. Four anther layers visible (Ep, En, ML and T). 3-4) MMCs divide, giving rise to 4-5) Meiotic Cells (MC). 6-8) Tetrads (Tt) appear concentrically in contact with tapetum cells; central locule appears empty and middle layer (ML) becomes crushed. 9-10) Young microspores (YM) released from tetrads, middle layer (ML) completely degenerated. 11 & 13) Tapetum starts degenerating. Vacuolated microspores (VM) and vacuolated pollen (VP) formed. 15) Pollen Mitosis I, the tapetum is still present. 16) Anther dehiscence. Septum has degenerated leaving two anther locules; stomium still remains intact. b) Comparison between barley (Optic) and wheat (Cadenza) anther and pollen development. Sp: Sporogenous Tissue; Ep: Epidermis; En: Endothecium; ML: Middle Layer; T: Tapetum; L: Lacunae; StR: Stomium Region; MMC: Microspore Mother Cells; Tt: Tetrads; YM: Young Microspores; VM: Vacuolate Microspores; VP: Vacuolate Pollen; MC: Meiotic Cell; St: stomium. Scale bar: 0.02mm.

Figure 6. Anther specific Transcription Factors expression patterns by qRT-PCR analysis.

a) *TaMS1*, b) *TaMYB26* c) *TaDYT1*. SC: Sporogenous Cells; Sc-t: Sporogenous Cells-tapetum generation; MMC: Microspore Mother Cells; MC: Meiotic Cells; Td: Tetrads; Ym: Young Microspores; VP: Vacuolated Pollen; MtI: Mitosis I.

Figures

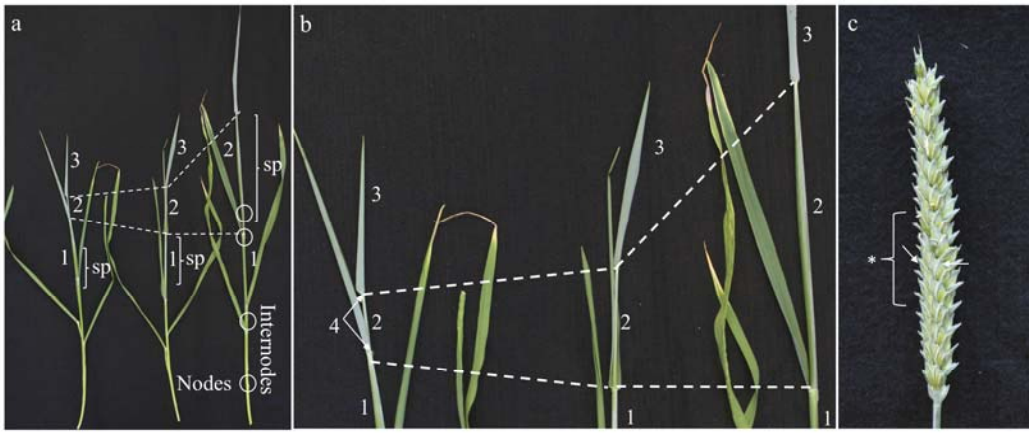

Figure 1. Cadenza Last Flag Sheath development.

a) Three tillers at different stages of development showing different last flag sheath extension, sp indicates the spike position within the pseudostem. White circles show the nodes. b) Close up view of last flag and last sheath at three different elongation stages. c) Close up image of wheat spike indicating the middle area used for sample collection for sectioning and qRT-PCR. 1: PLS (Previous Last Sheath); 2: LS (Last Sheath); 3: Last Flag; 4: Auricle; sp: Spike Position; *: Spike middle region for sample collection; White arrows indicates spikelet 1 and 2 position, which were the only spikelets used for collection.

a

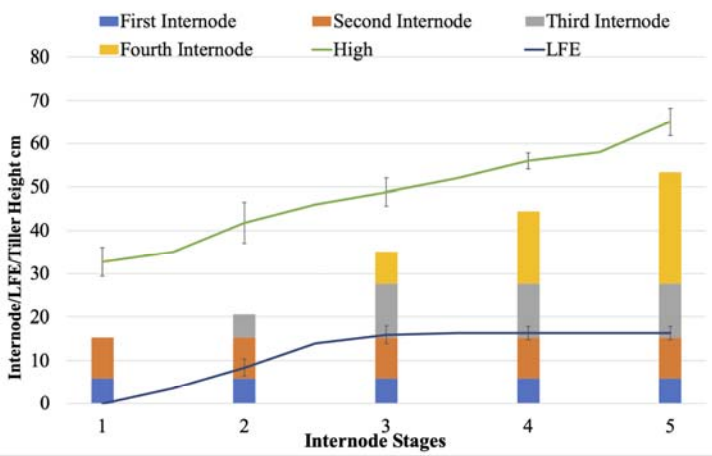

b

	Internode 1	Internode 2	Internode 3	Internode 4	Tiller Height	LFE
Stage 1	5.87+/-1.93 cm	9.5+/-0.57 cm			32.75+/-3.3 cm	0-3.5 cm
Stage 2	5.87+/-1.93 cm	9.5+/-0.57 cm	5.25+/-1.25 cm		41.75+/-4.71 cm	8.37+/-1.97 cm
Stage 3	5.87+/-1.93 cm	9.5+/-0.57 cm	12.25+/-1.7 cm	7.5+/-1.08 cm	48.87+/-3.19 cm	16+/-2.04 cm
Stage 4	5.87+/-1.93 cm	9.5+/-0.57 cm	12.25+/-1.7 cm	16.87+/-2.83 cm	56+/-1.87 cm	16.37+/-1.6 cm
Stage 5	5.87+/-1.93 cm	9.5+/-0.57 cm	12.25+/-1.7 cm	25.75+/-0.86 cm	65.07+/-3.16 cm	16.37+/-1.6 cm

Figure 2. Cadenza morphological development.

a) Internode elongation stages were determined by measuring internode elongation every 3 days. Tiller height (green line) and last flag elongation (blue line) was also measured. b) Five internode stages were created, starting from two fully elongated internodes (interode stage1), until four fully elongated internodes (internode stage 5). Tiller height increased steadily from stage 1 until 5, reaching a maximum of 65.1 ±3.2 cm. Last Flag Elongation (LFE) appeared between stage 1 and 2 and reached maximum elongation at stage 3.

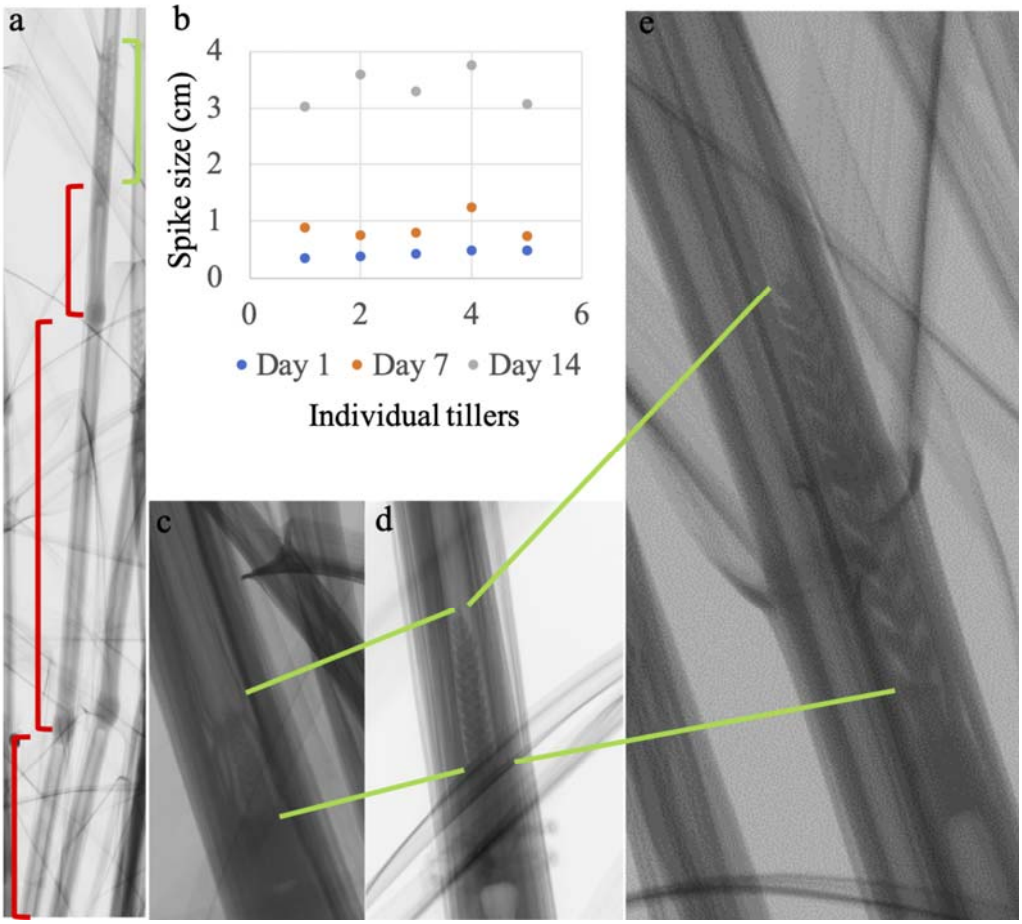

Figure 3. Cadenza internode and spike size development.

a) Internode elongation contribution to the spike upward movement (red brackets). b) Spike measurement started on day 48 after sowing (Zadock stage 30; spikes were around 0.5 cm long). a, c-e) μCT analysis of Cadenza spikelets. Spike size increase was observed over the following 14 days, spikes were up to 1.2 cm and >3 cm after 7 and 14 days respectively. c-e) Spike observed after c) day 1, d) day 7, and e) day 14.

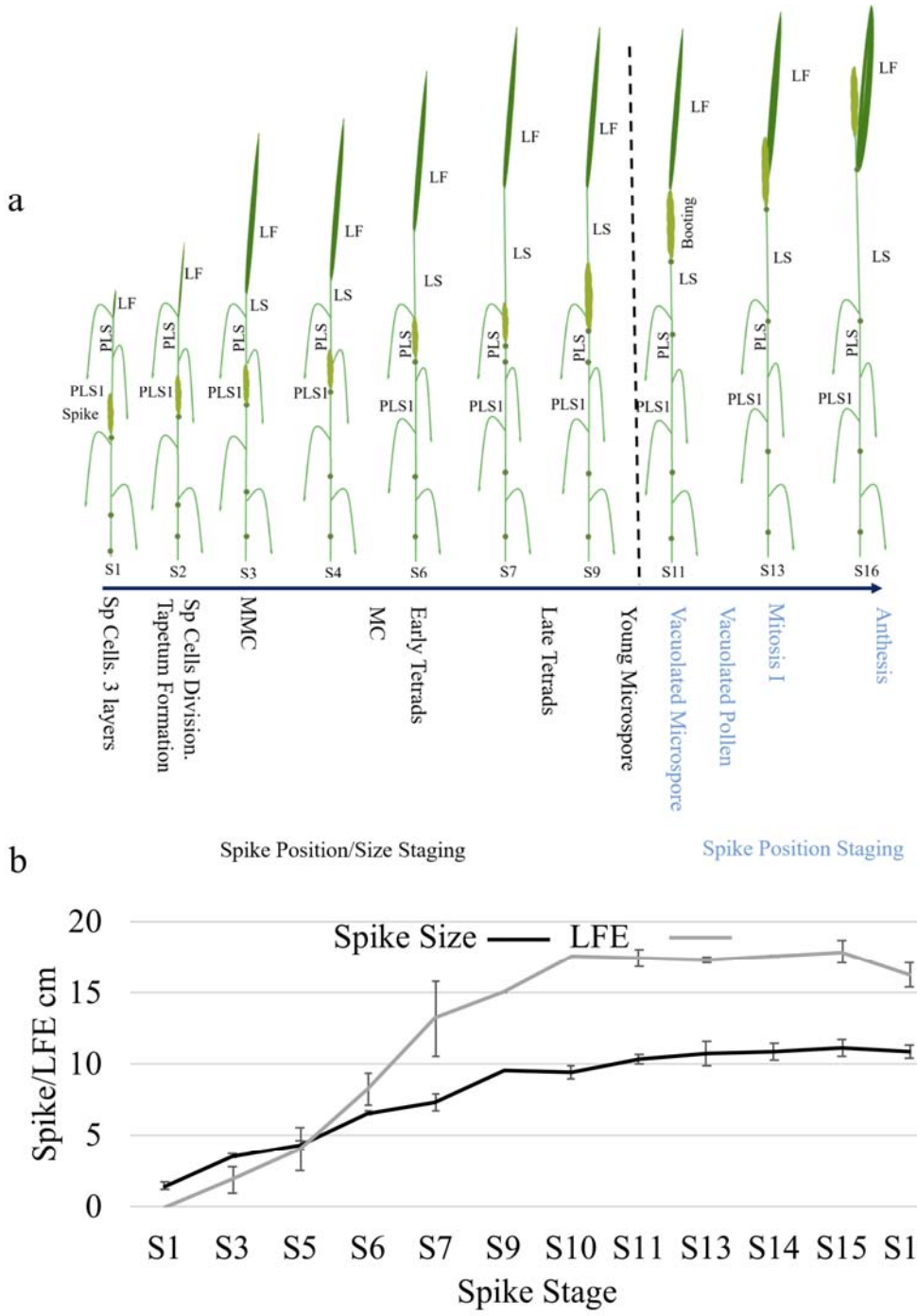

Figure 4. Cadenza spike position stages and spike size/last flag elongation (LFE) progression.

a) Spike position was divided into 16 stages, from early development, just before spike enters the "prior to previous last sheath" (PLS1) spike stage 1, until the spike is completely emerged, peduncule is elongated and anthers enter anthesis (spike stage 16). These 16 stages were linked to spike position within the pseudostem. b) Spike stage/spike size correlation. Spike position and spike size showed a close correlation

from stage 1 until stages 9-10. From stage 9-10 the spike ceased growing and remained unchanged.

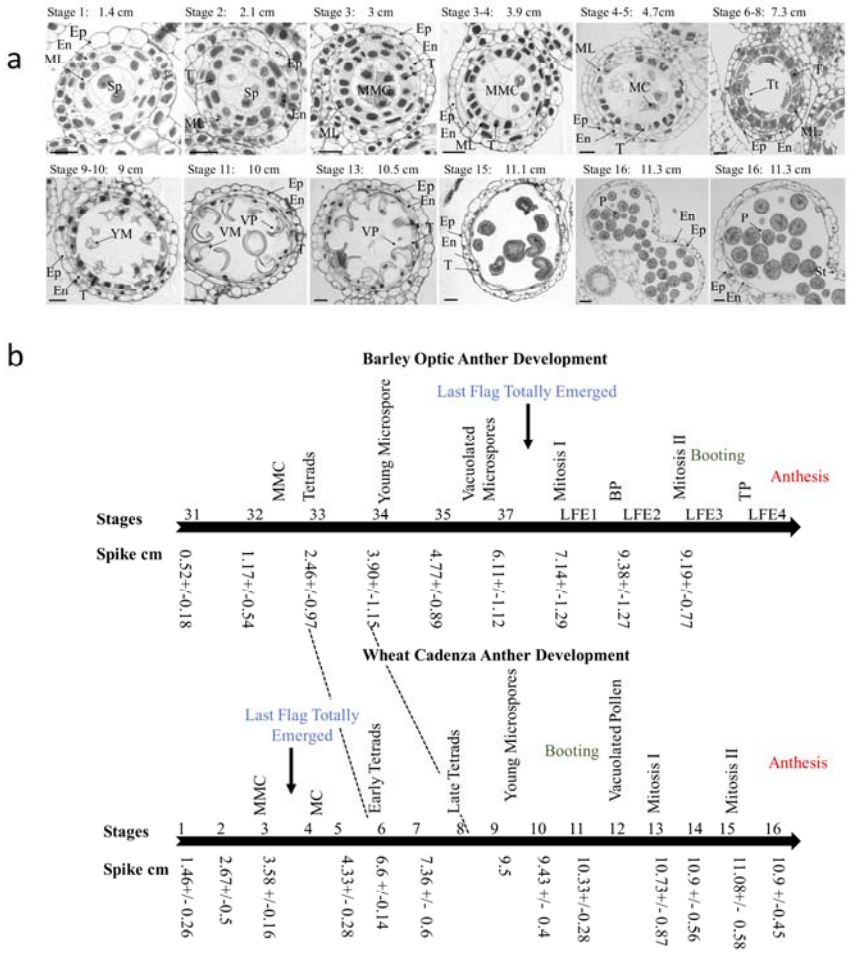

Figure 5. Developmentally staged Cadenza anther transverse sections.

a) Stages 1-16 of Cadenza anther development. 1) Sporogenous stage; three anther layers are visible (arrow; Ep, En and ML), sporogenous cells occupy the central region of the locule. 2) Sporogenous cells divide. Three anther layers clearly visible; start of tapetum formation (T). 3) Microspore Mother Cells (MMC) evident. Four anther layers visible (Ep, En, ML and T). 3-4) MMCs divide, giving rise to 4-5) Meiotic Cells (MC). 6-8) Tetrads (Tt) appear concentrically in contact with tapetum cells; central locule appears empty and middle layer (ML) becomes crushed. 9-10) Young microspores (YM) released from tetrads, middle layer (ML) completely degenerated. 11 & 13) Tapetum starts degenerating. Vacuolated microspores (VM) and vacuolated pollen (VP) formed. 15) Pollen Mitosis I, the tapetum is still present. 16) Anther dehiscence. Septum has degenerated leaving two anther locules; stomium still remains intact. b) Comparison between barley (Optic) and wheat (Cadenza) anther and pollen development. Sp: Sporogenous Tissue; Ep: Epidermis; En: Endothecium; ML: Middle Layer; T: Tapetum; L: Lacunae; StR: Stomium Region; MMC: Microspore Mother Cells; Tt: Tetrads; YM: Young Microspores; VM: Vacuolate Microspores; VP: Vacuolate Pollen; MC: Meiotic Cell; St: stomium. Scale bar: 0.02mm.

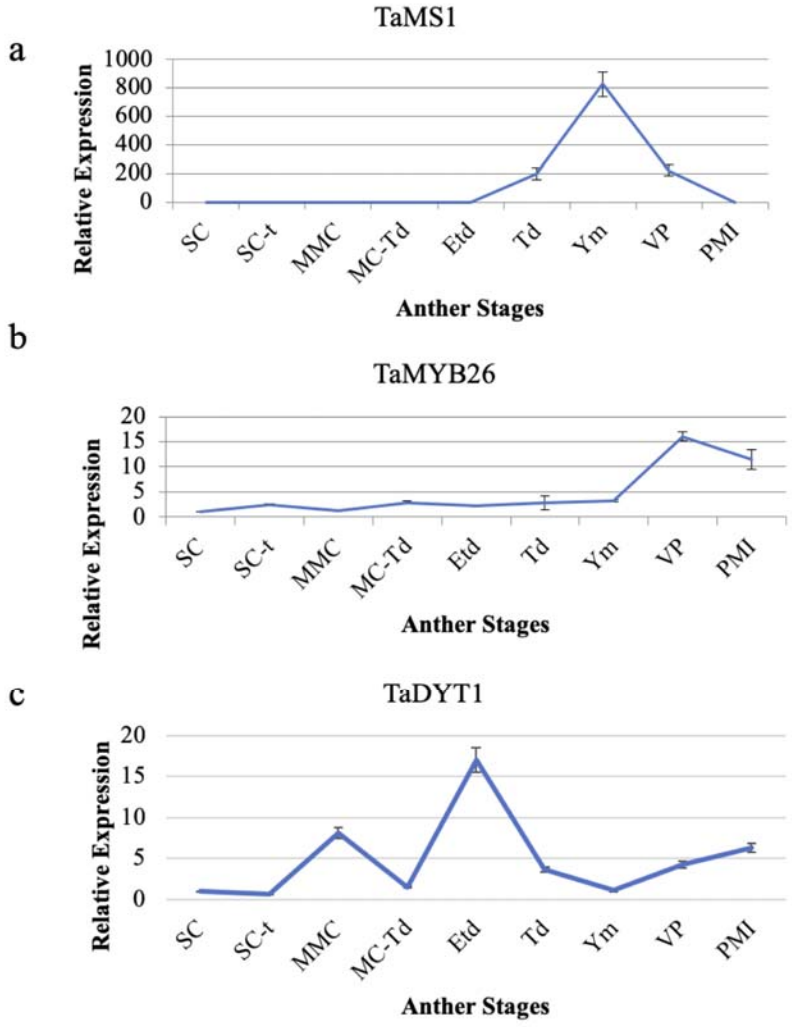

Figure 6. Anther specific Transcription Factors expression patterns by qRT-PCR analysis. a) *TaMS1*, b) *TaMYB26* c) *TaDYT1*. SC: Sporogenous Cells; Sc-t: Sporogenous Cells-tapetum generation; MMC: Microspore Mother Cells; MC: Meiotic Cells; Td: Tetrads; Ym: Young Microspores; VP: Vacuolated Pollen; MtI: Mitosis I.